MOLECULAR AND CELLULAR BIOLOGY, Oct. 1984, p. 1999–2009
0270-7306/84/101999-11$02.00/0

Vol. 4, No. 10

Cell Surface Expression of v-*fms*-Coded Glycoproteins Is Required for Transformation

MARTINE F. ROUSSEL, CARL W. RETTENMIER, A. THOMAS LOOK, AND CHARLES J. SHERR*

Divisions of Tumor Cell Biology and Hematology/Oncology, St. Jude Children's Research Hospital, Memphis, Tennessee 38101

Received 2 May 1984/Accepted 13 July 1984

The viral oncogene v-*fms* encodes a transforming glycoprotein with in vitro tyrosine-specific protein kinase activity. Although most v-*fms*-coded molecules remain internally sequestered in transformed cells, a minor population of molecules is transported to the cell surface. An engineered deletion mutant lacking 348 base pairs of the 3.0-kilobase-pair v-*fms* gene encoded a polypeptide that was 15 kilodaltons smaller than the wild-type v-*fms* gene product. The in-frame deletion of 116 amino acids was adjacent to the transmembrane anchor peptide located near the middle of the predicted protein sequence and 432 amino acids from the carboxyl terminus. The mutant polypeptide acquired N-linked oligosaccharide chains, was proteolytically processed in a manner similar to the wild-type glycoprotein, and exhibited an associated tyrosine-specific protein kinase activity in vitro. However, the N-linked oligosaccharides of the mutant glycoprotein were not processed to complex carbohydrate chains, and the glycoprotein was not detected at the cell surface. Cells expressing high levels of the mutant glycoprotein did not undergo morphological transformation and did not form colonies in semisolid medium. The transforming activity of the v-*fms* gene product therefore appears to be mediated through target molecules on the plasma membrane.

Retroviral oncogenes, acquired by recombination between viruses and protooncogenes found in the DNA of normal cells, encode proteins which morphologically transform cultured cells and induce tumors in animals. Several of the known viral oncogene products appear to affect cell growth by mechanisms which mimic the response of cell surface receptors to regulatory polypeptide hormones (or growth factors). For example, the product of the v-*sis* oncogene is homologous and possibly identical to the A chain of platelet-derived growth factor (8, 37) so that cells acquiring v-*sis* elaborate an autoendocrine signal. In contrast, the v-*erb*B gene encodes a glycoprotein closely related to a portion of the epidermal growth factor receptor (9) and may provide receptor signals in the absence of the extracellular ligand. It appears, then, that aberrant hormone or receptor signals at the plasma membrane can stimulate uncontrolled cell proliferation, leading to subsequent tumor formation.

The v-*fms* oncogene of the Susan McDonough strain of feline sarcoma virus (SM-FeSV) encodes a glycoprotein (1, 31) which is predicted to be an integral transmembrane protein (13; C. J. Sherr, S. J. Anderson, C. W. Rettenmier, and M. F. Roussel, *in* G. F. Vande Woude, W. Topp, A. J. Levine, and J. D. Watson [ed.], *Cancer Cells, vol. 2. Oncogenes and Viral Genes*, in press). Potential sites for glycosylation cluster in regions amino-terminal to the putative transmembrane anchor peptide, whereas carboxyl-terminal regions distal to the anchor sequence show striking homology to enzymes with tyrosine-specific protein kinase activity (13). Tyrosine-specific phosphorylation of the v-*fms*-coded glycoproteins themselves has been detected under certain assay conditions in immune complex kinase assays performed in vitro (3). However, only serine and threonine were phosphorylated in the glycoproteins metabolically labeled in vivo (3). In transformed cells, most v-*fms*-coded polypeptides remain internally sequestered and appear to be blocked in their intracellular transport through the Golgi complex (2). The internal sequestration of the glycoprotein is associated with reorganization of intermediate filaments. The major form of the v-*fms* glycoprotein is characteristic of molecules that remain within the endoplasmic reticulum, since it contains mannose-rich, N-linked oligosaccharide chains lacking fucose and sialic acid. A minor population of molecules undergoes further remodeling of its carbohydrates, acquiring terminal sugars in the Golgi complex; some of the processed molecules appear at the cell surface and can be detected by surface radiolabeling of intact cells or by immunofluorescence techniques (2). The polypeptides on the plasma membrane are presumed to be oriented with their amino-terminal portions outside of the cell and their carboxyl-terminal kinase domains interior to the plasma membrane (13; Sherr et al., in press).

It has not yet been possible to determine whether transformation is due to the vast majority of v-*fms*-coded polypeptides which are internally sequestered within transformed cells or to the minor population of glycoproteins on the plasma membrane. We have now engineered a nontransforming deletion mutant of the v-*fms* gene which encodes a smaller form of the glycoprotein that exhibits the in vitro tyrosine-specific protein kinase activity characteristic of wild-type v-*fms*-coded molecules. The mutant glycoprotein was not processed to mature forms of the molecule containing complex N-linked oligosaccharide chains and was not detected at the cell surface, suggesting that the plasma membrane is the site of action of the transforming glycoprotein.

MATERIALS AND METHODS

Preparation of an SM-FeSV deletion mutant. A 10-kilobase-pair *Eco*-RI fragment containing the complete 8.5-kilobase-pair SM-FeSV provirus cloned into a bacteriophage λ vector (7) was excised and recloned in two orientations at the *Eco*-RI site of the plasmid pBR322. Figure 1 shows a restriction map of the parental plasmid (pSM-FeSV) and

* Corresponding author.

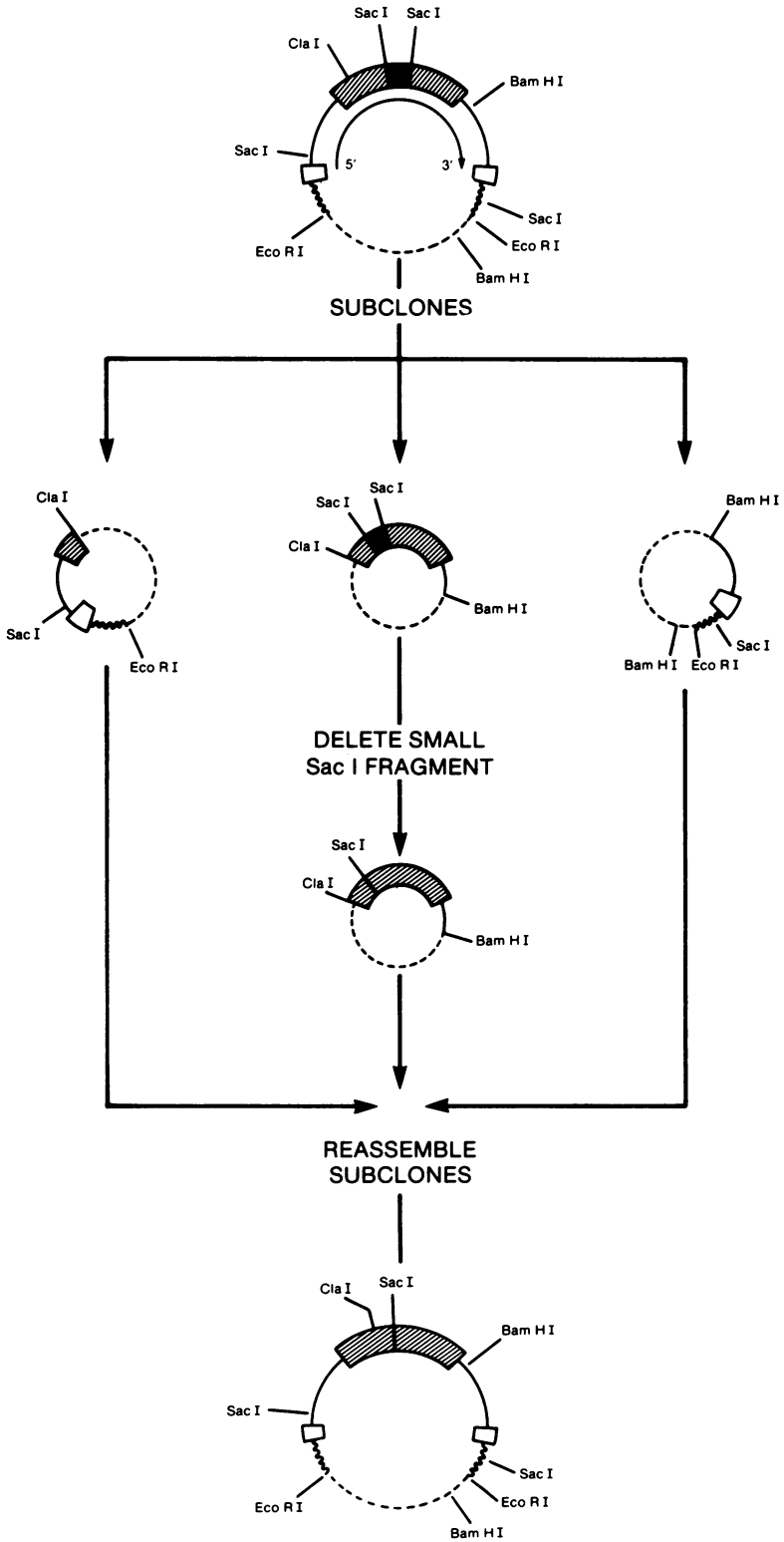

FIG. 1. Construction of a ΔpSM-FeSV DNA deletion mutant. The parental pSM-FeSV DNA is shown at the top. The viral long terminal repeat sequences are indicated by unshaded boxes, and the v-*fms* gene is indicated by the shaded rectangle. The location of the sequences deleted in the formation of ΔpSM-FeSV DNA is designated by the solid shaded area between the *Sac*I sites. Mink cellular sequences which flank the complete provirus are indicated by wavy solid lines, and vector sequences (pBR322) are indicated by the dashed line. The 5′ to 3′ orientation of the provirus with respect to viral RNA is indicated. Three subclones representing different, nonoverlapping portions of pSM-FeSV DNA are shown below the parental DNA construct. After deletion of the small *Sac*I fragment, the v-*fms* gene was reconstructed by inserting the *Cla*I-*Bam*HI fragment into the plasmid (shown at the left) containing 5′ long terminal repeat and v-*fms* sequences. A recloned plasmid containing the deleted v-*fms* gene was restricted with *Bam*HI, and a *Bam*HI fragment containing the 3′ SM-FeSV sequences (from the plasmid shown at the right) was inserted to generate ΔpSM-FeSV (bottom).

summarizes the construction of a deletion mutant (ΔpSM-FeSV) lacking a 348-base-pair segment of the v-*fms* gene. In brief, three subclones of pSM-FeSV were cloned in pBR322. The clone containing the major portion of the v-*fms* gene was digested with *Sac*I, and the small *Sac*I fragment was eliminated by reclosure. An intact provirus was then reconstructed, first by reconstituting the v-*fms* gene by ligation at the *Cla*I site and then by the addition of the *env* and long terminal repeat sequences 3′ to the single proviral DNA *Bam*HI site. Plasmids containing the appropriate deletion were mapped with restriction enzymes. Bona fide supercoiled ΔpSM-FeSV DNA was purified by extraction, banded isopycnically in cesium chloride, and desalted by gel filtration on Sepharose CL2B (Pharmacia Fine Chemicals, Piscataway, N.J.).

Transfection of NIH/3T3 cells. pSM-FeSV and ΔpSM-FeSV DNAs were assayed by transfection with the calcium phosphate precipitation method (12) as modified by Lowy et al. (21). In brief, 35-mm petri dishes were seeded with 3×10^5 cells one day before transfection, resulting in cells at 80% confluency the following day. Fresh medium was added 4 h before transfection. The test DNA, usually at 0.01 to 0.5 μg per plate, was added to 5 μg of sheared carrier NIH/3T3 DNA and suspended in 190 μl of solution containing 137 mM NaCl, 5 mM KCl, 0.7 mM Na_2HPO_4, 6 mM dextrose, and 20 mM HEPES (*N*-2-hydroxyethylpiperazine-*N*′-2-ethanesulfonic acid) at pH 6.92. The DNA was then precipitated for 30 min at room temperature by the addition of 1 M $CaCl_2$ in 0.01 M HEPES buffer, pH 5.5, to a final concentration of 10 M and then added to the culture. After 18 h of incubation with the DNA precipitate, the cells were trypsinized and seeded into three 60-mm dishes. With pSM-FeSV DNA, microscopic foci of transformed cells appeared within 5 to 8 days after transfection.

Cotransfection experiments were performed with a plasmid (pSV2) containing the dominant selectable marker, *eco gpt*; transfected colonies were selected in hypoxanthine-aminopterin-thymidine medium containing mycophenolic acid (24) before metabolic labeling or cell sorting experiments. To allow the spread of SM-FeSV genomes in transfected cultures, cotransfection was also performed with pSM-FeSV DNA and proviral DNA from a molecularly cloned, amphotropic murine leukemia virus (pA-MuLV). Transfected culture supernatants, shown to produce infectious virus with a test for virion-associated, RNA-dependent DNA polymerase, were filtered and used to infect rat NRK cells. Virus infection, polymerase assays, and titration of focus-forming SM-FeSV were performed as described previously (32) with 10-fold serial dilutions of virus-containing culture supernatants.

Metabolic radiolabeling of glycoproteins, preparation of cell lysates, and immunoprecipitatation. Metabolic radiolabeling medium consisted of Dulbecco modified Eagle medium supplemented with 2% dialyzed fetal calf serum. Subconfluent cell cultures in 75-cm^2 flasks were incubated for 1 h at 37°C either in 2 ml of methionine-free medium containing 1.0 mCi of L-[^{35}S]methionine (1,200 Ci/mmol) or in 2 ml of Dulbecco modified Eagle medium containing D-[2-^{3}H]mannose (15 Ci/mmol). An additional 5 ml of complete medium was then added, and the incubations were continued for an additional 2h. For metabolic labeling in the presence of tunicamycin, cultures were incubated in methionine-free medium containing 25 μg of drug per ml for 30 min before the addition of L-[^{35}S]methionine for an additional 30 min. Monolayers were lysed in RIPA buffer (50 mM Tris-hydrochloride [pH 7.4] containing 150 mM NaCl, 20 mM EDTA, 1% Triton X-100, 1% sodium deoxycholate, and 0.1% sodium dodecyl sulfate [SDS]) with 2% Aprotinin (Sigma Chemical Co., St. Louis, Mo.) and 1 mM phenylmethylsulfonyl fluoride as protease inhibitors. Immunoprecipitation was carried out in RIPA buffer with protein A-Sepharose CL-4B (Pharmacia) as the immunoadsorbant. Labeled proteins were separated on 7.5% polyacrylamide slab gels containing 0.1% SDS (18) and analyzed by fluorography. Apparent molecular weights of the proteins were estimated from their electrophoretic mobilities relative to those of marker protein standards.

Peptide mapping. Metabolically radiolabeled polypeptides in polyacrylamide gel slices were oxidized with performic acid and digested with L-(tosylamido 2-phenyl) ethyl chloromethyl ketone-treated trypsin as previously described (26). Eluted peptides were separated in two dimensions on cellulose-coated thin-layer plates (20 by 20 cm; EM Laboratories, Elmsford, N.Y.) by electrophoresis at 1,000 V for 20 min in acetic acid–formic acid–water (15:5:80; pH 1.9), followed by ascending chromatography in 1-butanol–pyridine–acetic acid–water (65:50:10:40) containing 7% (wt/vol) 2,5-diphenyloxazole. Dried plates were exposed to Kodak XAR-5 film for fluorography.

Immune complex kinase assay. Subconfluent cultures in 75-cm^2 flasks were lysed in 2 ml of RIPA buffer, and the nuclei were removed by centrifugation. To prepare immune complexes, 1 ml of lysate was incubated with 10 μl of polyvalent rat antiserum to v-*fms*-coded glycoproteins for 30 min at 22°C and then overnight at 4°C. Protein A-Sepharose was added, and the immune complexes were collected by centrifugation, washed five times with RIPA buffer containing 2 mM EDTA, and then washed twice with 50 mM Tris-hydrochloride (pH 7.4). Kinase reactions were initiated by adding 10 μl of 50 mM HEPES (pH 7.4) containing 10 mM $MnCl_2$ and 10 μCi of [γ-^{32}P]ATP (7,000 Ci/mmol). The precipitates were gently suspended and incubated 10 min at 30°C. Reactions were terminated by the addition of electrophoresis sample buffer (62.5 mM Tris-hydrochloride [pH 6.8] containing 3% SDS, 10% glycerol, and 50 mM dithiothreitol) and heating at 100°C for 2 min. Products were separated by electrophoresis in SDS-polyacrylamide gels and detected by autoradiography of the dried gel slab.

Monoclonal antibodies and antiserum. Polyvalent antiserum was raised in Osborn-Mendel rats inoculated with SM-FeSV-transformed NRK cells (29). Monoclonal antibodies were previously prepared by fusing the spleen from a responding animal to rat myeloma cells (1). Two monoclonal antibodies described previously, SM5.15.4 and SM3.19.4 (both γ1 isotype), were used for cell surface immunofluorescence and immunoblotting studies, respectively (see below). An additional monoclonal antibody, SM2.6.3 (γ2a isotype), was derived by similar methods and was also used in surface staining studies.

Immunoblotting analysis. Cell lysis, electrophoresis, and transfer of proteins from polyacrylamide gels to nitrocellulose were performed as previously described (1). The filters were preadsorbed in buffer A (0.15 M NaCl, 0.05 M Tris-hydrochloride [pH 7.4], 5 mM EDTA, 0.25% swine skin gelatin, 0.05% Nonidet P-40) for 60 min at room temperature. The filters were incubated for 30 min at 4°C with 10 μg of rat monoclonal antibody per ml, washed twice in buffer A, and incubated for 2 h at 4°C in buffer A containing 10 μg of rabbit antibody (immunoglobulin G fraction) to rat immunoglobulin G per ml. The filters were washed as above and incubated for 30 min at room temperature in buffer A containing 0.2 μCi of ^{125}I-labeled protein A (30 μCi/mg;

Amerham Radiochemicals, Arlington Heights, Ill.) per ml. The filters were then washed three times in buffer A adjusted to 1.0 M NaCl and 0.4% Sarkosyl (Sigma) and three times in distilled water, dried, and subjected to autoradiography.

Immunofluorescence analysis by flow cytometry. Subconfluent cell cultures were released from the plastic substrate by incubation for 20 min in Ca^{2+}- and Mg^{2+}-free phosphate-buffered saline (PBS) containing 0.6 mM EDTA, followed by a 5-min treatment with 10 μg of buffered trypsin (GIBCO Laboratories, Grand Island, N.Y.). The cells were collected by centrifugation and suspended in staining medium (Dulbecco modified Eagle medium containing 5% fetal calf serum, 10 mM HEPES, and 2 mM sodium azide), and 50-μl samples, each containing 10^6 cells, were incubated for 30 min at 4°C with 10 μg of monoclonal antibody or isotype-matched, control rat myeloma protein. The cells were washed three times and resuspended at the same concentration in staining medium containing a titered excess of affinity-purified, fluorescein isothiocyanate-conjugated goat antibody to rat immunoglobulin G (Tago Inc., Burlingame, Calif.). After incubation for 30 min at 4°C, the stained cells were washed three times and resuspended in 0.5 ml of staining medium containing 0.25 mM propidium iodide. Cells were analyzed at a rate of 500 cells per sec on an EPICS-V flow cytometer (Coulter Electronics, Hialeah, Fla.) with a laser output of 800 mW at 488 nm. Dead cells labeled with propidium iodide were excluded from the analysis (15). Fluorescein fluorescence was detected with a 510-nm interference filter, followed by a 525/40 band-pass filter. Frequency distribution profiles of the $\log_{10}$ fluorescence of 20,000 cells per sample were plotted, assigning a modal value of 1.0 to the cells stained with control myeloma protein. The control profile was identical to autofluorescence measured in the absence of antisera. Transfected NIH/3T3 cells were sorted into negative and positive subpopulations based on their fluorescence profile, and 25,000 cells, sorted in 35-mm petri dishes containing Dulbecco modified Eagle medium and 10% fetal calf serum, were grown up and analyzed.

RESULTS

The v-*fms* deletion mutant is inactive in transformation. Plasmids containing either wild-type (pSM-FeSV) or altered (ΔpSM-FeSV) proviral DNA sequences were tested for their ability to transform NIH/3T3 cells in a DNA transfection assay. Figure 2 shows that the two DNA constructs differ only with respect to a region of 348 nucleotides 5′ to the

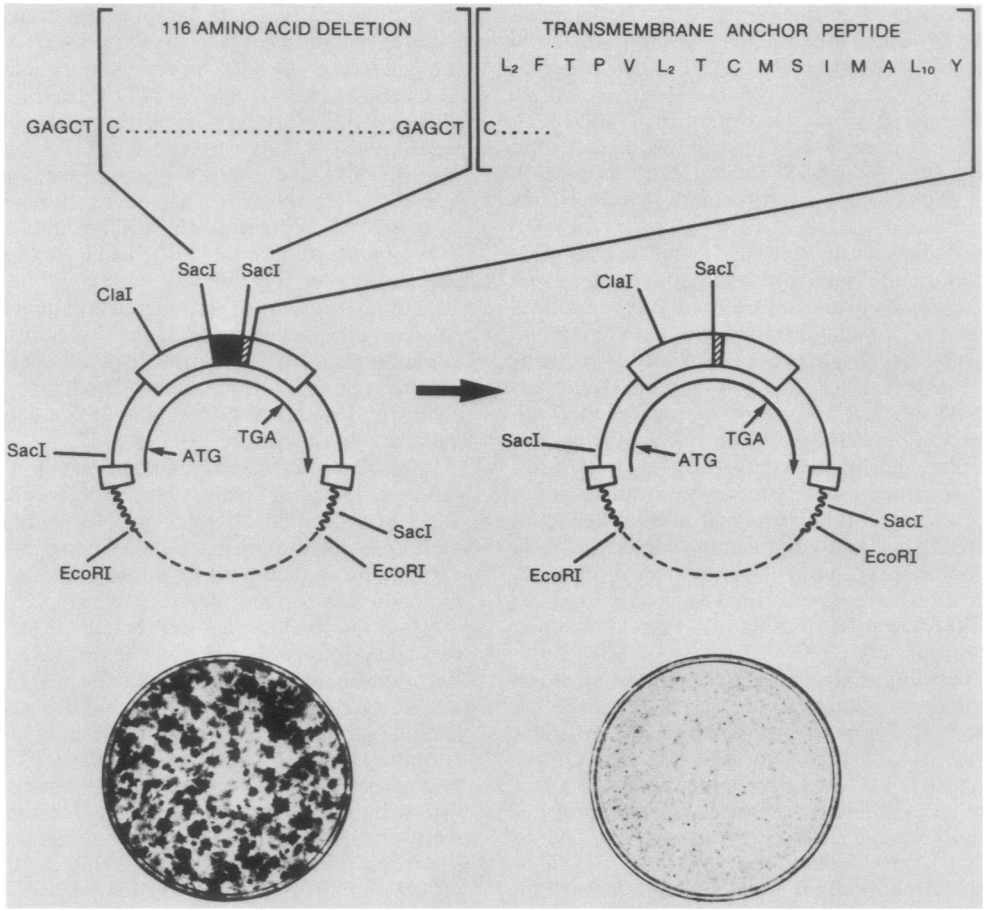

FIG. 2. Transforming activity of pSM-FeSV and ΔpSM-FeSV DNA. Restriction maps of the two plasmids shown in the center designate the location of *Sac*I sites used in deleting v-*fms* sequences and define the position of the adjacent sequence encoding the transmembrane anchor peptide. The initiation (ATG) and termination (TGA) codons of the open reading frame encoding the *gag-fms* fusion protein are indicated. The solid line 5′ to the v-*fms* gene defines the *gag* sequences. The deletion restores the first leucine codon of the 26-amino-acid, hydrophobic anchor peptide. Amino acid abbreviations are as follows: A, alanine; C, cysteine; F, phenylalanine; I, isoleucine; L, leucine; M, methionine; P, proline; S, serine; T, threonine; V, valine; and Y, tyrosine. NIH/3T3 cells transfected with 0.03 μg of pSM-FeSV DNA (left) or with 0.2 μg of ΔpSM-FeSV DNA (right) and stained with Giemsa 21 days later are shown at the bottom.

sequence encoding the putative hydrophobic membrane anchor peptide of the v-*fms* glycoprotein. Although the 3′ *Sac*I site used to delete the 348-nucleotide fragment occurs within the first leucine codon of the anchor peptide, this codon is restored in ΔpSM-FeSV DNA, leaving the anchor peptide intact. When wild-type pSM-FeSV DNA was tested in the transfection assay, numerous microscopic foci of transformed cells were detected within 5 days after transfection, and macroscopic foci were visible by 10 days. Figure 2 (bottom left) shows a representative culture transfected with 30 ng of pSM-FeSV DNA and stained with Giemsa 21 days later. Transfection with serial dilutions of DNA showed that the number of foci was a linear function of pSM-FeSV DNA dose within the range of 0.01 to 0.1 μg of DNA per culture and that the efficiency of focus formation in this dose range was ca. 2,000 focus forming units per μg of plasmid DNA. By contrast, foci of transformed cells were not detected with mutant ΔpSM-FeSV DNA at DNA doses of up to 1 μg per culture dish (Fig. 2, bottom right). These results show that proviral DNA containing the deletion in the v-*fms* gene is at least three orders of magnitude less active than wild-type DNA in this transformation assay.

To increase the sensitivity of the transformation assay, NIH/3T3 cells were cotransfected with pSM-FeSV proviral DNA and a second plasmid (pA-MuLV) containing proviral DNA of a replication-competent, amphotropic murine leukemia virus. It was reasoned that as many as 80% of the cells which took up DNA would acquire both proviruses (25) and would generate infectious FeSV that would spread through the culture and produce additional foci of transformed cells. Indeed, cotransfection with both plasmids generated visible foci within 3 days and resulted in completely transformed cultures within 8 days. When filtered supernatants from the transformed NIH/3T3 cultures were assayed for infectious transforming virus by titration of rat NRK cells, more than 2×10^5 U of focus forming virus per ml were detected. Even under these conditions, cotransfection of NIH/3T3 cells with mutant ΔpSM-FeSV and pA-MuLV DNAs neither generated detectable foci nor yielded competent transforming virus in the supernatants of the infected cultures.

To test whether NIH/3T3 cells transfected with ΔpSM-FeSV DNA produced a variant glycoprotein, it was first necessary to select those cells which acquired the nontransforming DNA. We therefore performed cotransfection experiments with ΔpSM-FeSV and the dominant selectable marker, *eco gpt*, and selected *eco gpt*-positive colonies in hypoxanthine-aminopterin-thymidine medium containing mycophenolic acid (24). These experiments were performed both in the presence or absence of pA-MuLV DNA. Colonies transfected with wild-type pSM-FeSV and *eco gpt* DNA underwent transformation in the presence of the selective media. Again, cotransfection of mutant ΔpSM-FeSV DNA with *eco gpt* in the presence or absence of pA-MuLV did not yield transformed colonies. Cells containing pSM-FeSV DNA formed colonies in agar (cloning efficiency, >40%), whereas cells derived by transfection with ΔpSM-FeSV DNA and *eco gpt* did not. As shown below, cells containing ΔpSM-FeSV express an altered v-*fms* gene product. Hence, the in-frame deletion of 116 amino acids renders this protein inactive as a transforming gene product.

The mutant v-*fms* gene encodes a variant glycoprotein. Because the formation of SM-FeSV involved the recombination of oncogene sequences into the *gag* gene of feline leukemia virus (7), SM-FeSV RNA specifies a polyprotein with amino-terminal residues encoded by *gag* sequences and carboxyl-terminal amino acids encoded by the v-*fms* gene (4, 29, 35). The primary translation product ($gP180^{gag\text{-}fms}$) is cotranslationally glycosylated (1, 31) and then proteolytically cleaved to yield an amino-terminal *gag*-coded polypeptide ($p55^{gag}$) and a carboxyl-terminal glycoprotein ($gp120^{fms}$) specified by the v-*fms* gene (4, 29). The v-*fms*-coded glycoprotein contains mannose-rich, N-linked oligosaccharide chains which, during the intracellular transport of the protein, are remodeled to complex oligosaccharides containing fucose and sialic acid (2). The latter product ($gp140^{fms}$) can be recognized by a greater apparent molecular weight in SDS-containing polyacrylamide gels (1, 2).

Cells containing either pSM-FeSV or ΔpSM-FeSV DNA, together with the *eco gpt* selectable marker, were incubated with [^{35}S]methionine, and detergent lysates were analyzed for products which could be precipitated with antibodies directed to v-*fms*-coded antigens. Figure 3A (lane 1) shows the typical pattern of v-*fms* polypeptides in transformed cells. These include $gP180^{gag\text{-}fms}$, $gp120^{fms}$, and $gp140^{fms}$. In cells containing DNA from the SM-FeSV deletion mutant (lane 2), the polyprotein $\Delta gP165^{gag\text{-}fms}$, which could also be precipitated by antiserum to *gag*-coded antigens, had an apparent molecular weight which was 15 kilodaltons smaller than the corresponding wild-type product. The mutant fusion protein was processed to a glycoprotein ($\Delta gp105^{fms}$) which was also ca. 15 kilodaltons smaller than $gp120^{fms}$. Hence, ΔpSM-FeSV codes for proteins of reduced molecular weights, which is consistent with the in-frame deletion of 116 amino acids. However, no analog of $gp140^{fms}$ was detectable in phenotypically flat cells containing ΔpSM-FeSV. Immunoprecipitation of the culture medium revealed no evidence for secretion of either the mutant or wild-type gene products.

The glycoprotein nature of these molecules was confirmed by labeling the polypeptides with [^{3}H]mannose. As shown in Fig. 3B, both the wild-type (lane 1) and mutant (lane 2) polypeptides were glycosylated. Although the mature form of the wild-type glycoprotein is inefficiently labeled with mannose due to remodeling of its N-linked oligosaccharide chains (1, 2), a low level of $gp140^{fms}$ was detected (lane 1). Consistent with the amino acid labeling experiment shown in Fig. 3A, no analog of $gp140^{fms}$ was seen in cells containing ΔpSM-FeSV.

The deleted amino acid sequences of ΔpSM-FeSV include three (of a total of 13) potential sites for the addition of N-linked oligosaccharide chains (13). To demonstrate that the alteration in molecular weight of the ΔpSM-FeSV gene products was due to differences in the polypeptides themselves and not simply in their carbohydrate moieties, metabolic radiolabeling with [^{35}S]methionine was performed in the presence of tunicamycin, an antibiotic which inhibits the addition of N-linked oligosaccharides. Figure 3C (lane 1) shows that the apparent molecular weights of the wild-type gene products were reduced in the presence of tunicamycin due to inhibition of glycosylation; in addition, no further processing of the unglycosylated polypeptides was observed, reflecting the fact that $gp140^{fms}$ and $gp120^{fms}$ differ only in the structure of their carbohydrate moieties. The size of the unglycosylated polypeptides encoded by ΔpSM-FeSV was 10 to 15 kilodaltons smaller than the corresponding wild-type molecules (Fig. 3C, lane 2), which was consistent with the expected deletion of 116 amino acids. However, due to the experimental error in estimating apparent molecular weights, we cannot exclude the possibility that one or more sites within the deleted region are glycosylated in wild-type molecules.

Another series of experiments took advantage of the fact

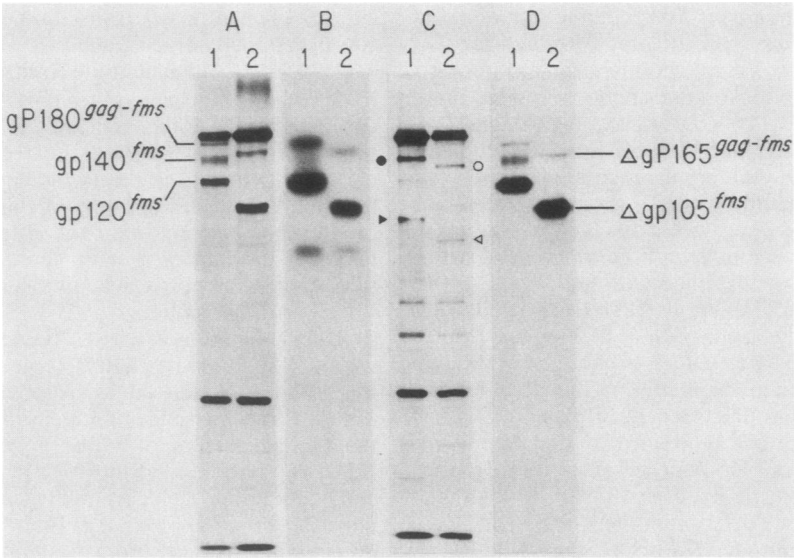

FIG. 3. Analysis of v-*fms*-coded glycoproteins in transfected NIH/3T3 cells. Each panel shows radiolabeled immunoprecipitated proteins obtained from cells containing wild-type pSM-FeSV (lanes 1) and from mutant ΔpSM-FeSV (lanes 2) constructs. (A) Proteins metabolically labeled with [^{35}S]methionine. The position of the wild-type glycoproteins in lane 1 are indicated at the left margin; the labeled band above gP180$^{gag\text{-}fms}$ is myosin. (B) Polypeptides metabolically labeled with [^{3}H]mannose. (C) [^{35}S]methionine-labeled polypeptides obtained from tunicamycin-treated cells; the positions of the unglycosylated polyproteins (circles) and cleavage products (triangles) are indicated by solid (wild-type) and open (mutant) symbols. Results of the in vitro protein kinase assay are shown in D. The positions of mutant glycoprotein molecules are indicated at the right margin.

that immune complexes containing v-*fms*-coded molecules exhibit an associated tyrosine-specific protein kinase activity which phosphorylates the v-*fms* products themselves (3). In these assays, all forms of the glycoprotein are active as in vitro substrates and become phosphorylated at tyrosine residues. As shown in Fig. 3D for wild-type v-*fms* transformants (lane 1), the addition of [γ-^{32}P]ATP to an immune complex kinase assay labeled gP180$^{gag\text{-}fms}$, gp120^{fms}, and gp140^{fms}. By contrast, when the assay was performed with immune complexes prepared from cells containing ΔpSM-FeSV DNA, ΔgP165$^{gag\text{-}fms}$ and Δgp105^{fms} were readily phosphorylated, whereas no gp140^{fms} analog was detected. Phosphoamino acid analyses demonstrated that both wild-type and mutant molecules were phosphorylated exclusively at tyrosine residues under the conditions of the in vitro assay (data not shown). Hence, the product of the mutant v-*fms* gene retains its associated protein kinase activity in vitro even though it is nontransforming in vivo.

To further compare the product of the deleted gene with the wild-type glycoprotein, the polypeptides were labeled with [^{35}S]methionine and subjected to tryptic peptide analyses. Figure 4 shows that Δgp105^{fms} (right panel) rendered a pattern of tryptic peptides which were indistinguishable from those of wild-type gp120^{fms} molecules (left panel). A mixing experiment in which labeled tryptic peptides of gp120^{fms} and Δgp105^{fms} were analyzed concurrently (center panel) confirmed that the two polypeptides could not be distinguished by these criteria. The absence of differences among the

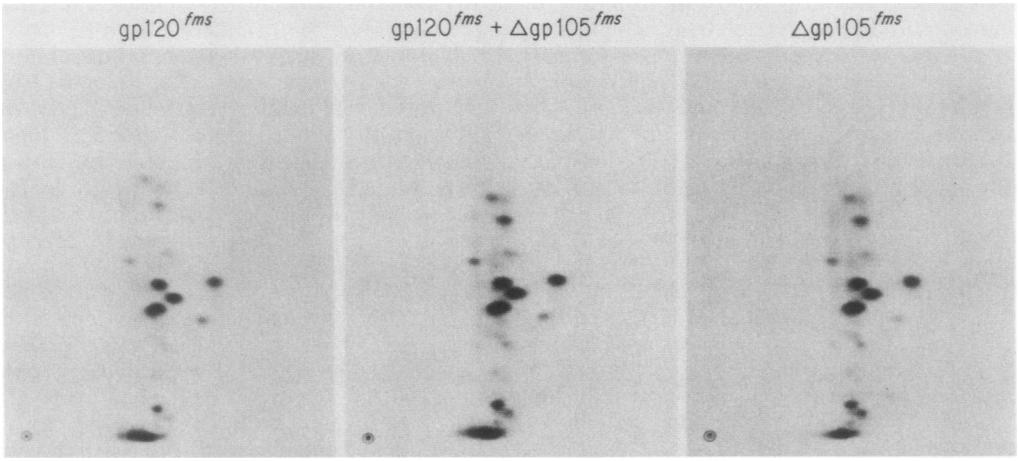

FIG. 4. Tryptic peptide analysis of [^{35}S]methionine-labeled, v-*fms*-coded glycoproteins. The proteins analyzed are noted at the top of each panel. The origin is at the lower left of each panel, with electrophoresis from left to right (anode at left) and ascending chromatography from bottom to top.

labeled peptides of wild-type and mutant glycoproteins is probably due to the fact that trypsin digestion was performed in polyacrylamide gel slices. The predicted deletion affects a single, large, labeled peptide which is very hydrophobic and would not be readily eluted from the gel. However, the results clearly show that gp120^{fms} and Δgp105^{fms} are chemically related molecules and strongly support the conclusion that Δgp105^{fms} was derived by an in-frame deletion which maintained the correct reading frame distal to the deleted sequence (a segment predicted to contain 432 amino acids).

The above experiments showed that cells containing ΔpSM-FeSV synthesize a truncated v-*fms*-coded product which is not converted to a mature form of the glycoprotein analogous to gp140^{fms}. To examine the possibility that the relative stability of Δgp105^{fms}, and hence its processing, might be affected by the deletion, the turnover of the mutant glycoprotein was studied (Fig. 5). Parallel cultures of NIH/3T3 cells containing either pSM-FeSV or ΔpSM-FeSV DNA were labeled for 15 min with [^{35}S]methionine and then incubated in fresh medium containing the nonradioactive amino acid precursor. Cell lysates prepared at various intervals were subjected to immunoprecipitation, and the v-*fms*-coded glycoproteins were examined. In cells transformed by pSM-FeSV, gp120^{fms} was detected after the 15-min labeling period, and as previously reported (2), a minority of gp120^{fms} molecules was processed to gp140^{fms} during the chase period (Fig. 5A). In cells containing ΔpSM-FeSV, Δgp105^{fms} molecules were not processed to mature glycoprotein forms, although their turnover was similar to that of wild-type gp120^{fms} molecules. As suggested by these analyses, immunoblotting experiments (Fig. 5B) showed that cells transfected by pSM-FeSV DNA (lane 1) and ΔpSM-FeSV DNA (lane 2) expressed gp120^{fms} and Δgp105^{fms}, respectively, at similar steady-state levels. These data show

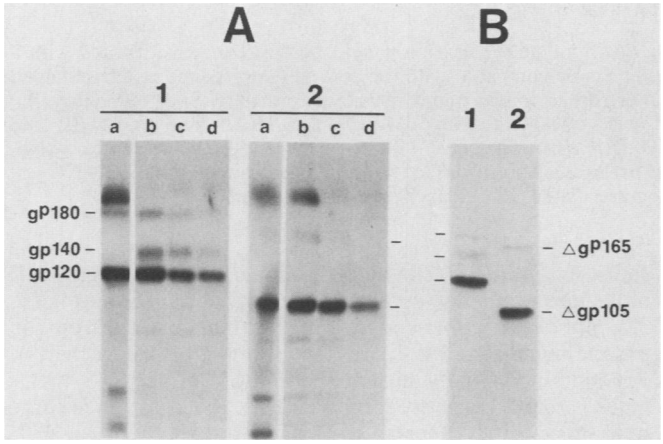

FIG. 5. Kinetic (A) and immunoblotting (B) analyses of v-*fms*-coded glycoproteins in wild-type pSM-FeSV (lane 1) and mutant ΔpSM-FeSV (lane 2) transfected NIH/3T3 cells. (A) Cells were pulse-labeled with [^{35}S]methionine for 15 min and then incubated in the presence of a 100-fold excess of nonradioactive methionine for chase intervals as follows: 0 h (a), 2 h (b), 4h (c), and 6 h (d). Radiolabeled v-*fms*-coded glycoproteins were immunoprecipitated, separated by SDS-gel electrophoresis, and detected by fluorography. The panel is a composite of lanes run on the same gel. The mobilities of the relevant bands are noted in the margins. (B) Equal quantities of protein from pSM-FeSV (lane 1) or ΔpSM-FeSV (lane 2) transfected cells were separated electrophoretically, transferred to nitrocellulose, and assayed with a monoclonal antibody (SM3.19.4) specific for a v-*fms*-coded epitope. Binding was detected by an indirect procedure with ^{125}I-labeled protein A.

that the failure to detect a mature form of the v-*fms*-coded glycoprotein in cells containing ΔpSM-FeSV (Fig. 3) is not due to an increased turnover of Δgp105^{fms}.

The mutant v-*fms* glycoproteins are not detected at the cell surface. Immunofluorescence experiments performed with fixed cells and either polyvalent antisera or monoclonal antibodies specific for v-*fms* gene products showed that a small proportion of v-*fms*-coded molecules were localized to the plasma membrane. Although gp120^{fms} is the major form of the glycoprotein in transformed cells, lactoperoxidase-catalyzed iodination of live cells showed that only gp140^{fms} molecules were detected at the cell surface (2). We have now used two different monoclonal antibodies (SM2.6.3 and SM5.15.4) to detect v-*fms*-coded epitopes on the surfaces of live transformed cells by fluorescence-activated flow cytometry. In control experiments, these two antibodies were shown to specifically react with v-*fms* transformants but not with untransformed control cells nor with cells transformed by another FeSV strain containing the oncogene v-*fes*. Positive fluorescence results were obtained with these antibodies with either mink, rat, or mouse cells transformed by SM-FeSV, showing that localization of the v-*fms*-coded glycoprotein to the cell surface was an intrinsic property of the molecule independent of the cell type and genetic background.

Figure 6 shows representative flow cytometric analyses of surface immunofluorescence detected with the monoclonal antibody SM2.6.3. Mink cells transformed by wild-type SM-FeSV uniformly showed high levels of antibody binding to surface molecules compared with the same cells stained with an isotype-matched rat myeloma protein (Fig. 6A). By contrast, NIH/3T3 cells cotransfected with pSM-FeSV and the dominant selectable marker *eco gpt* exhibited two subpopulations of cells based on binding of the same monoclonal antibody (Fig. 6B). One subpopulation, which accounted for 18% of the cells, showed a background level of fluorescence that was indistinguishable from the binding of the control myeloma protein. The second population, which accounted for 82% of the cells, showed specific binding of the antibody which was similar to that observed for v-*fms*-transformed mink cells. When fluorescence-activated sorting was used to individually separate the two subpopulations, cells showing no antibody binding were found to exhibit a phenotypically flat, contact-inhibited growth pattern, whereas the antibody-binding subpopulation was morphologically transformed. The fluorescence-negative flat cells could not be subcloned in agar (cloning efficiency, <1%), whereas the cells with detectable antibody binding gave rise to continuously growing agar colonies (cloning efficiency, >40%). Representative transformed NIH/3T3 subclones expressed SM-FeSV-coded proteins and showed uniformly high levels of antibody binding to surface molecules.

We assumed that the population of nonfluorescent cells seen in Fig. 6B represented those which had acquired the dominant selectable *eco gpt* marker in the absence of pSM-FeSV DNA (25). To test this possibility, cells were cotransfected with pSM-FeSV, *eco gpt*, and pA-MuLV DNA. Under these conditions, cells acquiring the selectable marker in the absence of the transforming pSM-FeSV DNA could be subsequently infected with the transforming virus. A more homogeneous population of fluorescent cells was obtained when the transforming virus was allowed to spread through the culture (Fig. 6C). These experiments suggest, then, that fluorescence-activated flow cytometry can be used to identify and select cells of the transformed phenotype, based on surface expression of v-*fms*-coded molecules.

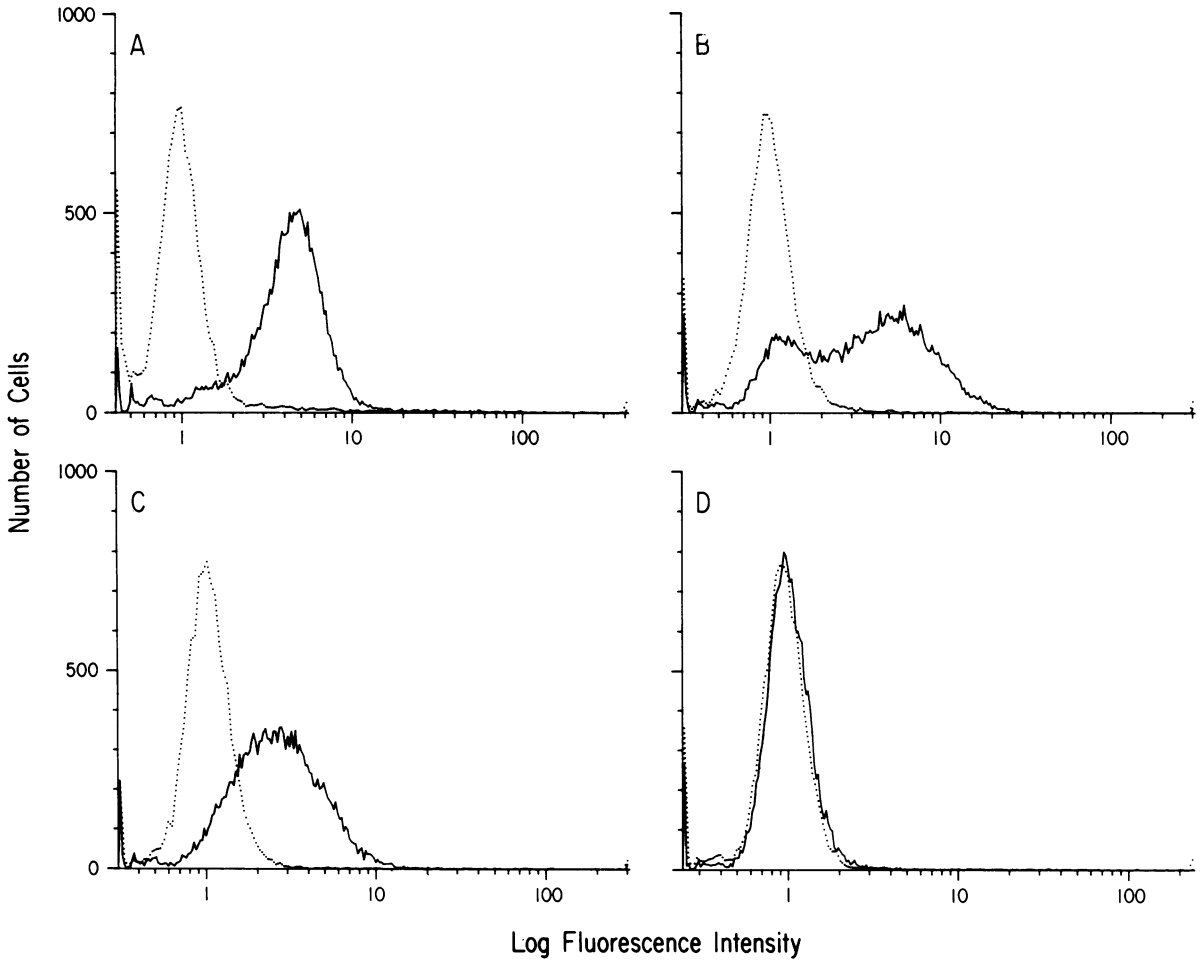

FIG. 6. Cell surface expression of v-*fms*-coded antigens detected by flow cytometry. In each panel, the fluorescence recorded with a monoclonal antibody (SM2.6.3) directed to a v-*fms*-coded epitope (solid line) was compared with the control fluorescence profile obtained with an isotype-matched rat myeloma protein (dotted line). The results shown are as follows: mink cells transformed by SM-FeSV virus (A); NIH/3T3 cells transfected with pSM-FeSV DNA and *eco gpt* (B); NIH/3T3 cells transfected with pSM-FeSV, pA-MuLV, and *eco gpt* (C); and NIH/3T3 cells transfected with ΔpSM-FeSV, pA-MuLV, and *eco gpt* (D). All cells transfected with *eco gpt* were grown in hypoxanthine-aminopterin-thymidine medium containing mycophenolic acid for 3 weeks before analysis of surface fluorescence. The cells analyzed in C and D were shown to be producing virus with an assay for supernatant virion-associated, RNA-dependent DNA polymerase.

Cells transfected by ΔpSM-FeSV and *eco gpt* in the presence or absence of pA-MuLV showed no v-*fms*-specific surface fluorescence. Figure 6D shows that the profile obtained with the SM2.6.3. monoclonal antibody was identical to that obtained with the control rat myeloma protein. Similar results were also obtained with monoclonal antibody SM5.15.4. To rule out the possibility that the lack of surface fluorescence of ΔpSM-FeSV-containing cells reflected the inability of these particular monoclonal antibodies to react with mutant v-*fms*-coded glycoproteins, the cells were labeled with [^{35}S]methionine, and lysates were subjected to immune precipitation (Fig. 7). Both monoclonal antibodies specifically precipitated gp120^{fms} and Δgp105^{fms}, indicating that the epitopes recognized by these two antibodies were expressed on mutant glycoprotein molecules. Thus, cells containing ΔpSM-FeSV neither express the transformed phenotype nor exhibit v-*fms* glycoproteins at their surface.

DISCUSSION

Few v-*fms*-coded glycoproteins are processed to mature gp140^{fms} molecules that appear at the surface of SM-FeSV-transformed cells (2). Indeed, in early studies, gp140^{fms} molecules were not detected by metabolic labeling (4, 29, 35), nor were v-*fms*-coded antigens demonstrated on the plasma membrane by fluorescent staining of fixed cells (1). Kinetic studies showed that the half-life of gp140^{fms} molecules is relatively short compared with gp120^{fms} which turns over more slowly. Hence, the steady-state level of gp120^{fms} in transformed cells is considerably higher than that of gp140^{fms}, and it seems likely that relatively few gp140^{fms} molecules appear at the cell surface at any time (2). Nevertheless, as shown here, the presence of the glycoprotein on the plasma membrane correlates with the transformed phenotype. As compared with wild-type v-*fms*-coded molecules, the truncated glycoprotein synthesized by the SM-FeSV deletion mutant was even more inhibited in its processing and transport, as judged by the failure to undergo remodeling of its N-linked oligosaccharides and to reach the cell surface. The deletion could have itself included a domain necessary for transport through the Golgi complex or, alternatively, may have altered processing signals elsewhere in the molecule. Mutants of vesicular stomatitis G protein,

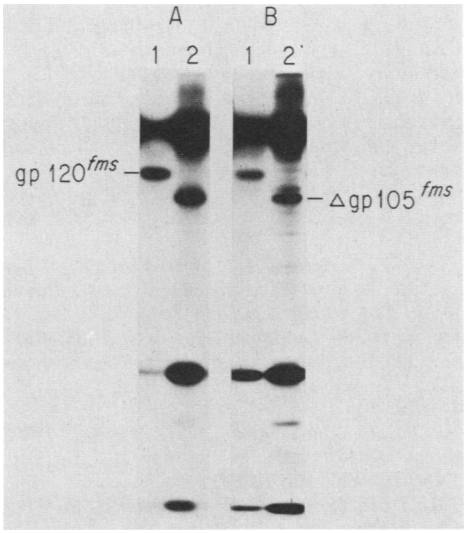

FIG. 7. Immune precipitation of v-*fms*-coded glycoproteins with monoclonal antibodies. NIH/3T3 cells transfected with DNAs from pSM-FeSV (lanes 1) or ΔpSM-FeSV DNA (lanes 2) were labeled for 30 min with [^{35}S]methionine, and detergent lysates were precipitated with monoclonal antibodies SM2.6.3. (A) or SM5.15.4 (B). Because the monoclonal antibodies do not bind protein A, immune precipitates were prepared with protein A-Sepharose beads coated with goat antiserum to rat immunoglobulin G. The heavy labeled band near the top of each lane is myosin, which obscures the position of the *gag-fms* polyproteins; gp140^{fms} is not visualized in a 30-min labeling period (Fig. 5 and reference 2). The positions of gp120^{fms} and Δgp105^{fms} are indicated.

when altered at carboxyl-terminal sequences adjacent to the membrane anchor sequence, were also found to be retarded in intracellular transport and no longer localized to the plasma membrane (28).

Immune complexes containing v-*fms*-coded glycoproteins exhibit a tyrosine-specific protein kinase activity under some assay conditions (3; C. W. Rettenmier, unpublished data) but not others (27, 36). By contrast, the glycoproteins metabolically labeled in vivo with $^{32}P_i$ contain phosphoserine and lesser amounts of phosphothreonine but lack detectable phosphotyrosine (3). Although the 200 carboxyl-terminal amino acids of the glycoprotein were predicted to show close homology to retrovirus-transforming proteins that specify tyrosine-specific protein kinase activity (13), it is not known whether the glycoproteins themselves act as enzymes or, rather, serve as efficient substrates for a coprecipitating kinase in vitro. In the studies reported here, the wild-type v-*fms* gene products were active as substrates in immune complexes and were phosphorylated only at tyrosine. The amino acids deleted from the mutant glycoprotein were derived from a region of the polypeptide nearly 300 residues amino-terminal to the kinase domain and did not affect the in vitro enzyme activity. If kinase activity proves to be an intrinsic property of the v-*fms*-coded glycoprotein, then the enzymatic function in itself must be insufficient for transformation. The possibility that the deletion ablated an additional functional domain unrelated to kinase activity but required for transformation cannot be formally excluded. However, we suggest that an interaction between the v-*fms*-coded glycoprotein and specific target molecules at the plasma membrane is important in transformation.

Viral tyrosine-specific protein kinases such as the prototype Rous sarcoma virus transforming protein pp60^{src} associate with the cytoplasmic surface of the plasma membrane in transformed cells (6, 17, 38). The v-*src* gene product is synthesized on free polyribosomes (19), is post-translationally modified by the covalent attachment of fatty acid (11, 30), and becomes membrane associated through its modified amino terminus (11, 16), thereby orienting the carboxyl-terminal kinase domain in the cytoplasm (20). Rous sarcoma virus mutants encoding pp60^{src} proteins that contain critical amino-terminal deletions are less tumorigenic in birds, suggesting that the association of pp60^{src} with the plasma membrane is important in transformation (16). Unlike pp60^{src}, the v-*fms*-coded product is synthesized as an integral transmembrane glycoprotein on membrane-bound polyribosomes and is then transported through the endoplasmic reticulum and Golgi complex to the cell surface. Although the carboxyl-terminal kinase domain of gp140^{fms} is oriented in the cytoplasm in a manner analogous to pp60^{src}, the amino-terminal half of the polypeptide is exteriorized at the cell surface and can be detected after lactoperoxidase-catalyzed radioiodination of intact cells or by live cell immunofluorescence (2). Analogous findings have been reported with the v-*erb*B-coded glycoprotein, the expression of which at the cell surface is correlated with transformation (5).

The presence of v-*fms*-coded glycoproteins at the cell surface can be used to select transformed cells from phenotypically normal ones by fluorescence-activated cell sorting. When NIH/3T3 cells were transfected with wild-type pSM-FeSV and a dominant selectable marker, *eco gpt*, a phenotypically flat subpopulation containing *eco gpt* alone and a morphologically transformed subpopulation containing pSM-FeSV and the selectable marker were obtained. The transformed population could be purified by flow cytometry and gave rise to cells which formed colonies in agar and uniformly expressed v-*fms*-coded antigens at the cell surface. Fluorescence-activated cell sorting might therefore be used to screen for morphologically revertant populations of SM-FeSV-infected cells which no longer express surface antigens. Conversely, it might be possible to select phenotypically flat cellular mutants which continue to express v-*fms* antigens but are refractory to transforming signals.

Relatively high levels of RNA encoded by the c-*fms* protooncogene are expressed late in mouse embryogenesis (22) and can be detected in both mouse and human placental trophoblasts (23) and in certain human tumors (33). However, the protein product of the c-*fms* locus has not been identified. To date, the only candidate is a 200-kilodalton polypeptide detected in normal mink cells with a single monoclonal antibody (2), and this protein has not been further characterized. Given the ability to detect tyrosine-specific protein kinase activity associated with the v-*fms* gene product in vitro, the simplest model is that the c-*fms* protooncogene is a member of a class of receptor genes that encode similar enzymatic functions. The latter include the epidermal growth factor receptor (34), now known to be homologous to the v-*erb* gene product (9), as well as the platelet-derived growth factor and insulin-like growth factor receptors, each of which exhibits an associated tyrosine-specific protein kinase activity (10, 14). If c-*fms* encodes a receptor, then antibodies to v-*fms*-coded epitopes expressed at the cell surface may have the potential of binding these molecules and mimicking ligand-mediated signals.

ACKNOWLEDGMENTS

We thank Carol Claus, Shawn Kramer, and Mathew Rebentisch for excellent technical assistance, David Kingsbury and Mary

Walker for critical comments on the manuscript, William R. Fields of Eli Lilly & Co. for a gift of mycophenolic acid, Douglas Lowy of the National Cancer Institute for pA-MuLV DNA, H. Bazin of the University of Brussels for rat myeloma proteins, and Robert Eisenman of Fred Hutchinson Cancer Center for the indirect immunoblot protocol.

This work was supported by Cancer Center (CORE) Grant CA21765 and by ALSAC. C.W.R. was supported by a Biomedical Research Support Grant (RR-05584-19) from the National Institutes of Health to St. Jude Children's Research Hospital.

LITERATURE CITED

1. **Anderson, S. J., M. Furth, L. Wolff, S. K. Ruscetti, and C. J. Sherr.** 1982. Monoclonal antibodies to the transformation-specific glycoprotein encoded by the feline retroviral oncogene v-*fms*. J. Virol. **44**:696–702.
2. **Anderson, S. J., M. A. Gonda, C. W. Rettenmier, and C. J. Sherr.** 1984. Subcellular localization of glycoproteins encoded by the viral oncogene v-*fms*. J. Virol. **51**:730–741.
3. **Barbacid, M., and A. V. Lauver.** 1981. Gene products of McDonough feline sarcoma virus have an in vitro-associated protein kinase that phosphorylates tyrosine residues: lack of detection of this enzymatic activity in vivo. J. Virol. **40**:812–821.
4. **Barbacid, M., A. V. Lauver, and S. G. Devare.** 1980. Biochemical and immunological characterization of polyproteins coded for by the McDonough, Gardner-Arnstein, and Snyder-Theilen strains of feline sarcoma virus. J. Virol. **33**:196–207.
5. **Beug, H., and M. J. Hayman.** 1984. Temperature-sensitive mutants of avian erythroblastosis virus: surface expression of the *erb*B product correlates with transformation. Cell **36**:963–972.
6. **Courtneidge, S. A., A. D. Levinson, and J. M. Bishop.** 1980. The protein encoded by the transforming gene of avian sarcoma virus ($pp60^{src}$) and a homologous protein in normal cells ($pp60^{proto\text{-}src}$) are associated with the plasma membrane. Proc. Natl. Acad. Sci. U.S.A. **77**:3783–3787.
7. **Donner, L., L. A. Fedele, C. F. Garon, S. J. Anderson, and C. J. Sherr.** 1982. McDonough feline sarcoma virus: characterization of the molecularly cloned provirus and its feline oncogene (v-*fms*). J. Virol. **41**:489–500.
8. **Doolittle, R. F., M. W. Hunkapiller, L. E. Hood, S. G. Devare, K. C. Robbins, S. A. Aaronson, and H. N. Antoniades.** 1983. Simian sarcoma virus *onc* gene, v-*sis*, is derived from the gene (or genes) encoding a platelet-derived growth factor. Science **221**:275–276.
9. **Downward, J., Y. Yarden, E. Mayes, G. Scrace, N. Totty, P. Stockwell, A. Ullrich, J. Schlessinger, and M. D. Waterfield.** 1984. Close similarity of epidermal growth factor receptor and v-*erbB* oncogene protein sequences. Nature (London) **307**:521–527.
10. **Ek, B., B. Westermark, A. Wasteson, and C. H. Heldin.** 1982. Stimulation of tyrosine-specific phosphorylation by platelet-derived growth factor. Nature (London) **295**:419–420.
11. **Garber, E. A., J. G. Krueger, H. Hanafusa, and A. R. Goldberg.** 1982. Only membrane-associated RSV *src* proteins have amino-terminally bound lipid. Nature (London) **302**:161–163.
12. **Graham, F. L., and A. J. Van der Eb.** 1973. Transformation of rat cells by DNA of human adenovirus 5. Virology **54**:536–539.
13. **Hampe, A., M. Gobet, C. J. Sherr, and F. Galibert.** 1984. Nucleotide sequence of the feline retroviral oncogene v-*fms* shows unexpected homology with oncogenes encoding tyrosine-specific protein kinases. Proc. Natl. Acad. Sci. U.S.A. **81**:85–89.
14. **Kasuga, M., Y. Zick, D. L. Blithe, M. Crettaz, and R. Kahn.** 1982. Insulin stimulates tyrosine phosphorylation of the insulin receptor. Nature (London) **298**:667–669.
15. **Kavathas, P., and L. A. Herzenberg.** 1983. Stable transformation of mouse L cells for human membrane T-cell differentiation antigens, HLA and B2 microglobulin: selection by fluorescence-activated cell sorting. Proc. Natl. Acad. Sci. U.S.A. **80**:524–528.
16. **Krueger, J. G., E. A. Garber, A. R. Goldberg, and H. Hanafusa.** 1982. Changes in aminoterminal sequences of $pp60^{src}$ lead to decreased in vivo tumorigenicity. Cell **28**:889–896.
17. **Krueger, J. G., E. Wang, E. A. Garber, and A. R. Goldberg.** 1980. Differences in the intracellular location of pp60*src* in rat and chicken cells transformed by Rous sarcoma virus. Proc. Natl. Acad. Sci. U.S.A. **77**:4142–4146.
18. **Laemmli, U. K.** 1970. Cleavage of structural proteins during the assembly of the head of bacteriophage T4. Nature (London) **227**:680–685.
19. **Lee, J. S., H. E. Varmus, and J. M. Bishop.** 1979. Virus-specific messenger RNAs in permissive cells infected with avian sarcoma virus. J. Biol. Chem. **254**:8015–8022.
20. **Levinson, A. D., S. A. Courtneidge, and J. M. Bishop.** 1981. Structural and functional domains of the Rous sarcoma virus transforming protein ($pp60^{src}$). Proc. Natl. Acad. Sci. U.S.A. **78**:1624–1628.
21. **Lowy, D. R., E. Rands, and E. M. Scolnick.** 1978. Helper-independent transformation by unintegrated Harvey sarcoma virus DNA. J. Virol. **26**:291–298.
22. **Müller, R., D. L. Slamon, E. D. Adamson, J. M. Tremblay, D. Müller, M. J. Cline, and I. M. Verma.** 1983. Transcription of c-*onc* genes c-ras^{ki} and c-*fms* during mouse development. Mol. Cell. Biol. **3**:1062–1069.
23. **Müller, R., J. Tremblay, E. D. Adamson, and I. M. Verma.** 1983. Tissue and cell type specific expression of two human c-*onc* genes. Nature (London) **304**:454–456.
24. **Mulligan, R. C., and P. Berg.** 1981. Selection for animal cells that express the *Escherichia coli* gene coding for xanthine-guanine phosphoribosyltransferase. Proc. Natl. Acad. Sci. U.S.A. **78**:2072–2076.
25. **Perucho, M., D. Hanahan, and M. Wigler.** 1980. Genetic and physical linkage of exogenous sequences in transformed cells. Cell **22**:309–317.
26. **Rettenmier, C. W., R. E. Karess, S. M. Anderson, and H. Hanafusa.** 1979. Tryptic peptide analysis of avian oncovirus *gag* and *pol* gene products. J. Virol. **32**:102–113.
27. **Reynolds, F. H., Jr., W. J. M. Van de Ven, J. Blomberg, and J. R. Stephenson.** 1981. Differences in mechanisms of transformation by independent feline sarcoma virus isolates. J. Virol. **38**:1084–1089.
28. **Rose, J. K., and J. E. Bergmann.** 1983. Altered cytoplasmic domains affect intracellular transport of the vesicular stomatitis virus glycoproteins. Cell **34**:513–524.
29. **Ruscetti, S. K., L. P. Turek, and C. J. Sherr.** 1980. Three independent isolates of feline sarcoma virus code for three distinct gag-x polyproteins. J. Virol. **35**:259–264.
30. **Sefton, B. M., I. S. Trowbridge, J. A. Cooper, and E. M. Scolnick.** 1982. The transforming proteins of Rous sarcoma virus, Harvey virus, and Abelson virus contain tightly bound lipids. Cell **31**:465–474.
31. **Sherr, C. J., L. Donner, L. A. Fedele, L. Turek, J. Even, and S. K. Ruscetti.** 1980. Molecular structure and products of feline sarcoma and leukemia viruses: relationship to FOCMA expression, p. 293–307. *In* W. D. Hardy, Jr., M. E. Essex, and A. J. McClelland (ed.), Feline leukemia virus. Elsevier/North-Holland Publishing Co., Amsterdam.
32. **Sherr, C. J., L. A. Fedele, L. Donner, and L. P. Turek.** 1979. Restriction endonuclease mapping of unintegrated proviral DNA of Snyder-Theilen feline sarcoma virus: localization of sarcoma-specific sequences. J. Virol. **32**:860–875.
33. **Slamon, D. J., J. B. deKernion, I. M. Verma, and M. J. Cline.** 1984. Expression of cellular oncogenes in human malignancies. Science **224**:256–262.
34. **Ushiro, H., and S. J. Cohen.** 1980. Identification of phosphotyrosine as a product of epidermal growth factor-activated protein kinase in A-431 cell membranes. J. Biol. Chem. **255**:8363–8365.
35. **Van de Ven, W. J. M., F. H. Reynolds, Jr., R. P. Nalewaik, and J. R. Stephenson.** 1980. Characterization of a 170,000-dalton polyprotein encoded by the McDonough strain of feline sarcoma virus. J. Virol. **35**:165–175.
36. **Veronese, F., G. J. Kelloff, F. H. Reynolds, Jr., R. W. Hill, and**

J. R. Stephenson. 1982. Monoclonal antibodies specific to transforming polyproteins encoded by independent isolates of feline sarcoma virus. J. Virol. **43**:896–904.

37. **Waterfield, M. D., G. T. Scrace, N. Whittle, P. Stroobant, A. Johnsson, A. Wasteson, B. Westermark, C.-H. Heldin, J. S. Huang, and T. F. Deuel.** 1983. Platelet derived growth factor is structurally related to the putative transforming protein $p28^{sis}$ of simian sarcoma virus. Nature (London) **304**:35–39.
38. **Willingham, M. C., G. Jay, and I. Pastan.** 1979. Localization of the avian sarcoma virus *src* gene product to the plasma membrane of transformed cells by electron microscopic immunocytochemistry. Cell **18**:125–134.